

# Single granule cells reliably discharge targets in the hippocampal CA3 network *in vivo*

Darrell A. Henze, Lucia Wittner and György Buzsáki

Center for Molecular and Behavioral Neuroscience, Rutgers University, The State University of New Jersey, 197 University Avenue, Newark, New Jersey 07102, USA

Correspondence should be addressed to G.B. (buzsaki@axon.rutgers.edu)

Published online: 15 July 2002, doi:10.1038/nn887

**Processing of neuronal information depends on interactions between the anatomical connectivity and cellular properties of single cells. We examined how these computational building blocks work together in the intact rat hippocampus. Single spikes in dentate granule cells, controlled intracellularly, generally failed to discharge either interneurons or CA3 pyramidal cells. In contrast, trains of spikes effectively discharged both CA3 cell types. Increasing the discharge rate of the granule cell increased the discharge probability of its target neuron and decreased the delay between the onset of a granule cell train and evoked firing in postsynaptic targets. Thus, we conclude that the granule cell to CA3 synapses are 'conditional detonators,' dependent on granule cell firing pattern. In addition, we suggest that information in single granule cells is converted into a temporal delay code in target CA3 pyramidal cells and interneurons. These data demonstrate how a neural circuit of the CNS may process information.**

Input from the dentate gyrus to the hippocampus is implicated in various physiological functions, such as memory and spatial representation<sup>1–3</sup>, and in pathological states such as epilepsy<sup>4–6</sup>. Neocortical information is conveyed to hippocampal CA3 pyramidal neurons both directly via the perforant path from the entorhinal cortex and indirectly by way of the mossy fibers of granule cells. A large number of granule cells (1 million in the rat<sup>7</sup>) innervate the 300,000 CA3 pyramidal cells via the mossy fibers with very limited convergence (~50 granule cells per pyramidal cell) and divergence (~14 pyramidal cells per granule cell<sup>8</sup>) via a specialized presynaptic giant mossy fiber bouton<sup>9</sup>. In addition, each granule cell innervates 40 to 50 CA3 interneurons via filopodial extensions that extend from the giant bouton and *en passant* boutons along the main mossy fiber axon<sup>10,11</sup>. The anatomical differentiation of mossy fiber synapses onto pyramidal cells and interneurons is associated with a functional segregation with respect to short-term and long-term plasticity<sup>12,13</sup>. Despite the wealth of knowledge about the anatomy and synaptic physiology of this system, nothing is known how granule cell activity influences the activity of CA3 targets in the intact network *in vivo*. This knowledge is important because models of hippocampal function assume that the mossy fiber synapse is a 'detonator' or 'teacher' synapse critical for directing the storage of information in the auto-associative CA3 network<sup>3,14</sup>. A detonator or teacher synapse strongly controls the activity of the postsynaptic target without need of coordinated input from other synapses onto the postsynaptic target<sup>14</sup>. The hypothesized deterministic firing of CA3 pyramidal cells by granule cells is assumed to provide the 'Hebbian' postsynaptic depolarization<sup>15,16</sup> required to strengthen the commissural/associational and/or perforant path inputs

to the activated CA3 pyramidal neurons. Although previous *in vitro* investigations have illuminated some important properties of the mossy fiber synapses (for review, see ref. 17), the conditions required to discharge CA3 neurons by granule cells in the intact brain have remained unexplored.

Our data demonstrate that spike transmission (a precise temporal relationship between single pre- and postsynaptic spikes) occurs between granule cells and their pyramidal cell and interneuron targets in area CA3. Spike transmission from a granule cell to CA3 was not observed for single spikes but instead required trains of spikes with the maximum spike transmission probability depending on the frequency of granule cell firing. Finally, physiological patterns of granule cell firing contain periods of high-frequency firing that effectively drove CA3 pyramidal cells and interneurons.

## RESULTS

We directly addressed the influence of granule cells on the activity of CA3 targets by recording *in vivo* from a population of potential targets in the CA3c region while controlling granule cell activity via intracellular current injection using a sharp microelectrode (ref. 18; Methods). The current injections allowed the arbitrary control of granule cell spiking, thus permitting us to dissociate the influence of single granule cell activity from background network drive. Multiple single units in area CA3c were recorded extracellularly and isolated using multichannel silicon probes and clustering analysis techniques (Methods). Individual units were identified as pyramidal cells or interneurons based on published criteria<sup>18–20</sup>. A plot of unit spike asymmetry (duration of the first half of the spike divided by the duration of the last

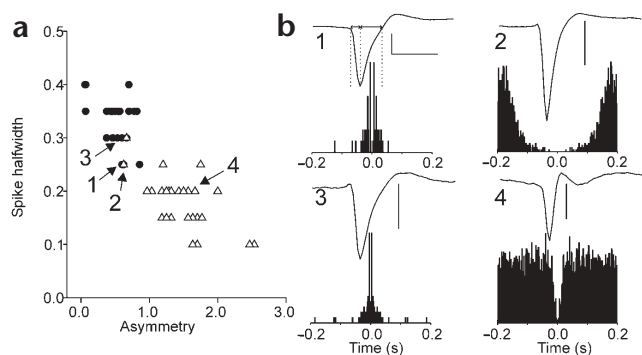


**Fig. 1.** Classification of extracellular units. **(a)** Extracellular unit waveform asymmetry (time from baseline to negative peak/time from negative peak to baseline, see horizontal arrows in **b1**) versus unit spike half-amplitude width. Closed circles and open triangles are putative pyramidal cells and interneurons, respectively. **(b)** Example wideband (1 Hz–8 kHz) unit waveforms and autocorrelograms that were used to confirm unit classification. The asymmetry measurement is illustrated with vertical dotted lines and horizontal arrows in **b1**. Pyramidal cells have wider and more asymmetric waveforms and a peak at short interspike intervals in the autocorrelogram. Interneurons have narrower and more symmetric waveforms and lack a peak at short interspike intervals in the autocorrelograms. The lettered arrows in **(a)** correspond to the subpanels in **(b)**. Scale bars: horizontal, 1 ms; vertical, 100  $\mu$ V, 50  $\mu$ V, 50  $\mu$ V, 25  $\mu$ V for **b1**, **2**, **3** and **4**, respectively.

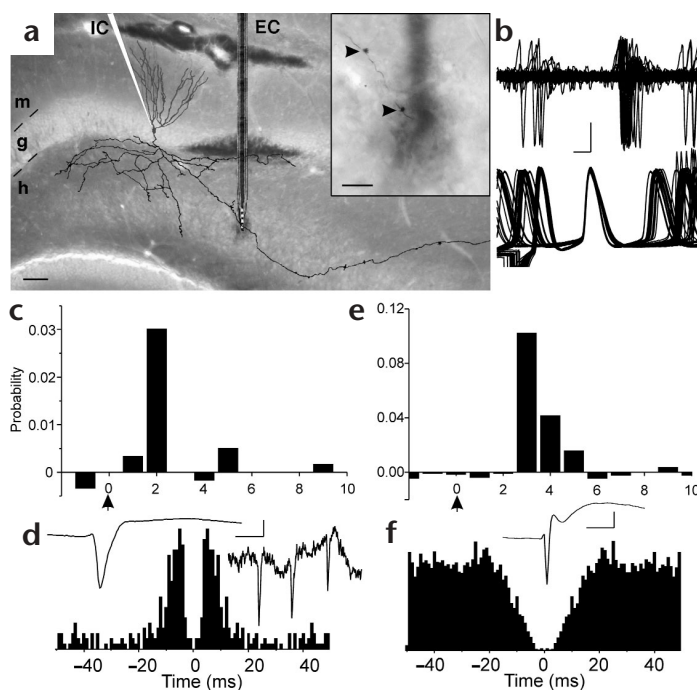
half) versus half-width resulted in a diagonal separation of units (Fig. 1a) that allowed unit identification when combined with the unit autocorrelograms (Fig. 1b). Putative pyramidal cells ( $n = 22$ ) had low mean firing rates outside the evoked activity ( $0.91 \pm 0.18$  Hz) and had wider, asymmetrical wideband waveforms ( $0.32 \pm 0.01$  ms half-width;  $0.52 \pm 0.05$  symmetry ratio). Four putative pyramidal cell units had enough spontaneous spikes for us to construct spike autocorrelograms, typical of pyramidal neurons<sup>19</sup> (Figs. 1b and 2d). Putative interneurons ( $n = 26$ ), on average, discharged faster ( $3.38 \pm 0.75$  Hz) and had narrower spikes ( $0.18 \pm 0.01$  ms half-width;  $1.46 \pm 0.09$  symmetry ratio), and the autocorrelograms did not show a peak at less than 10 ms (Figs. 1b and 2f). Ten neurons could not be classified into either category using these criteria.

Intracellularly evoked granule cell action potentials resulted in time-locked unit activity in a subset of target CA3c neurons (Fig. 2b). The fixed short latency of the unit activity indicated a monosynaptic connection between the granule cell and its CA3c targets<sup>19,21</sup>. Spike transmission, the occurrence of a precise time-locked spike by a postsynaptic cell following a spike in a presyn-

naptic cell, occurred between granule cells and CA3 targets in 37 of 69 rats. A connection was considered for detailed analysis when there was a significant peak in the cross-correlation in the 6 ms following the granule cell action potential (defined as over 3 standard deviations above the mean of the overall cross-correlation). Of the 37 rats with qualitatively observed spike transmission, 13 animals yielded 58 pairs with recordings of sufficient quality and length to generate unit clusters and quantify spike transmission probability (1–11 driven units per successful experiment). Twenty-two of the driven units were pyramidal cells (Fig. 2c and d), and 26 were interneurons (Fig. 2e and f). The average distance between the closest *en passant* or giant mossy fiber bouton and the probe (Fig. 2a, inset) was  $51.4 \pm 10.1$   $\mu$ m ( $\pm$  standard error of the mean, s.e.m.) for the 7 experiments in which mossy fibers were recovered anatomically.

On average, putative pyramidal cells had shorter and more precise spike transmission latencies than putative interneurons (Table 1). The spike transmission probability depended on the combined effect of granule cell discharge frequency and the number of spikes within the train (Fig. 3). Single granule cell spikes

**Fig. 2.** Spike transmission between a granule cell and its interneuron and pyramidal cell targets in CA3c. **(a)** Camera lucida reconstruction of a biocytin-labeled granule cell and the extracellular electrode track where spike transmission was observed. Scale bar, 50  $\mu$ m. m, molecular layer; g, granule cell layer; h, hilus; IC, intracellular electrode track; EC, extracellular electrode track. Inset, a higher-power view of the mossy fiber axon near the probe track. Arrowheads, mossy fiber boutons; scale bar, 20  $\mu$ m. **(b)** Superimposed ( $n = 60$ ) intracellularly evoked action potentials in a granule cell (bottom traces) and simultaneously recorded extracellular units (filtered 0.8–8 kHz). Note the time-locked response of a putative pyramidal cell to the granule cell action potentials. The granule cell was driven by 350 ms depolarizing steps. Scale bar, 1 ms, 25 mV, 75  $\mu$ V. **(c)** Cross-correlogram (shuffle corrected) expressed as probability (number of unit spikes per bin/total number of granule cell spikes) between the evoked granule cell action potentials and the activity of a putative CA3c pyramidal cell. The arrowhead indicates the peak time of the granule cell action potential. **(d)** Autocorrelogram of the pyramidal cell unit during non-evoked periods. Left inset, the average wide-band waveform of the pyramidal cell (high-pass filtered at 1 Hz). Scale bar, 1 ms, 20  $\mu$ V. Right inset, spontaneous complex burst of the pyramidal cell. Scale bar, 5 ms, 20  $\mu$ V. As in **(c)**, but for an isolated CA3 interneuron. **(e, f)** As in **(c, d)**, but the extracellular unit is a putative CA3c interneuron.



were generally ineffective, failing to show significant peaks in the cross-correlations in 54 of the 58 pairs (including 10 unidentified targets). However, high-frequency granule cell spike trains could result in spike transmission with a probability greater than 0.8 (pyramidal cells, 0.017 to 0.842; interneurons, 0.022 to 0.57). In the pair shown in Fig. 3a, the first action potential in the train failed to evoke extracellular spikes, whereas maximum spike transmission probability occurred following the fifth spike (putative pyramidal cell unit; maximum probability, 0.52). For 45 of the 48 identified pairs, spike transmission (a significant peak at 2–6 ms in the cross-correlation) required at least two presynaptic spikes. Subsequently, the maximum spike transmission probability occurred later in the train (Table 1; Fig. 3b), followed by a late train reduction in spike transmission probability. In the three remaining identified pairs (one pyramidal cell, two interneurons), the first spike probability was greater than or equal to later spikes (first spike probability, 0.26, 0.02, 0.30, respectively). The overall mean spike transmission probability was higher for the putative pyramidal cell targets than for putative interneurons, regardless of the changes over the course of the train ( $0.157 \pm 0.015$  versus  $0.050 \pm 0.004$ ;  $P < 0.00001$ ; two-way ANOVA).

The discharge frequency of the granule cell affected both discharge probability and the latency between the onset of the presynaptic train and postsynaptic firing. At 10 Hz, spike transmission probability was low, whereas at 100 Hz, it was high. In the pair shown in Fig. 4a, maximum probability occurred after the third to sixth spike. The combined effect of spike frequency and spike number in the granule cell resulted in a considerable time shift between the onset of the granule cell train and the maximum spike transmission probability (Fig. 4a, arrows). Figure 4b sum-

**Table 1. Granule cell–CA3 spike transmission dynamics.**

	Number of units	Mean latency (ms)	Mean precision (ms)	Mean spike number to maximum probability
Overall (including 10 unclassified units)	58	$2.94 \pm 0.066$	$1.01 \pm 0.041$	$4.82 \pm 0.51$
Pyramidal cell	22	$2.73 \pm 0.069^*$	$0.81 \pm 0.046^{**}$	$3.94 \pm 0.44$
Interneuron	26	$3.14 \pm 0.122^*$	$1.24 \pm 0.049^{**}$	$4.62 \pm 0.40$

\* $P < 0.01$ , \*\* $P < 0.00001$ , two-tailed *t*-tests (pyramidal cells versus interneurons). Latency was calculated between the peak of the granule cell action potential and the negative peak of the extracellular spike. Mean precision was calculated as the mean standard deviation of the latency from each driven unit.

marizes the effect of granule cell firing frequency on the time of maximum spike transmission probability ( $n = 5$ ) from the beginning of the train. For all pairs, the time between the onset of the presynaptic train and the time when highest spike transmission probability was reached decreased several-fold as a function of

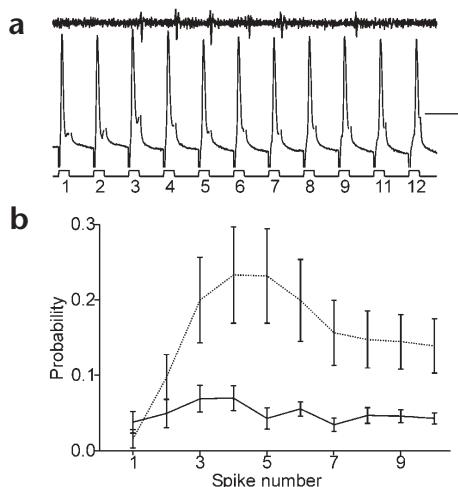


**Fig. 3.** Spike transmission dynamics. (a) Top, filtered (0.8–8 kHz) extracellular trace of a putative pyramidal cell. Middle, granule cell action potentials evoked by brief current injections at 100 Hz (artifacts digitally removed). Bottom, current injection pattern. Scale bar, top, 100  $\mu$ V; middle, 25 mV, 10 ms. (b) Spike transmission probability (shuffle-corrected probability of spike in 6 ms following intracellular spike) as a function of spike number in evoked 100 Hz train ( $\pm$  s.e.m.). Solid line, putative interneurons ( $n = 24$ ); dotted line, putative pyramidal cells ( $n = 21$ ).

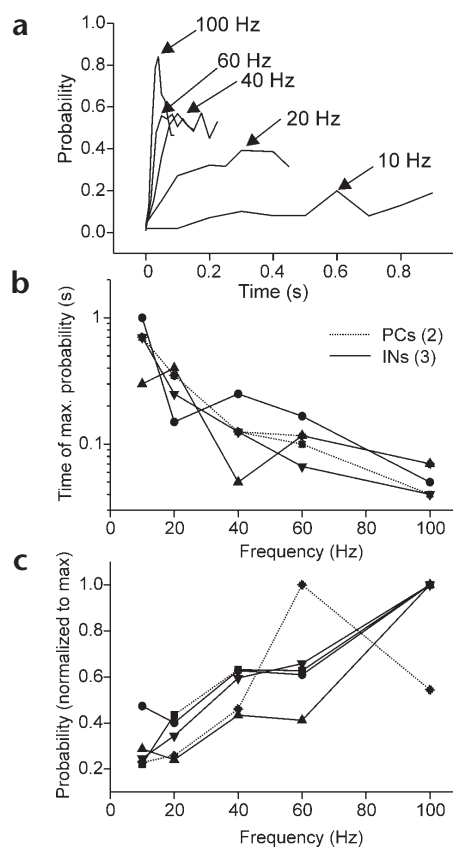


**Fig. 4.** Frequency dependence of granule cell–CA3 spike transmission. (a) Representative results of the effect of intratrain frequency on spike transmission probability for a putative pyramidal cell. (b) Time of maximum probability following onset of the granule cell spike train as a function of frequency for two pyramidal cells (dotted lines) and three interneurons (solid lines). As granule cell spiking frequency increases, the latency from the granule cell train onset of the maximum discharge probability of the postsynaptic unit decreases. (c) The maximum probability of spike transmission normalized across granule cell spike train frequencies for two pyramidal cells (dotted lines) and three interneurons (solid lines). The maximum probability of spike transmission was observed for the highest frequency (100 Hz) in 4 of 5 cells. The different symbols represent the different cells in (b) and (c).



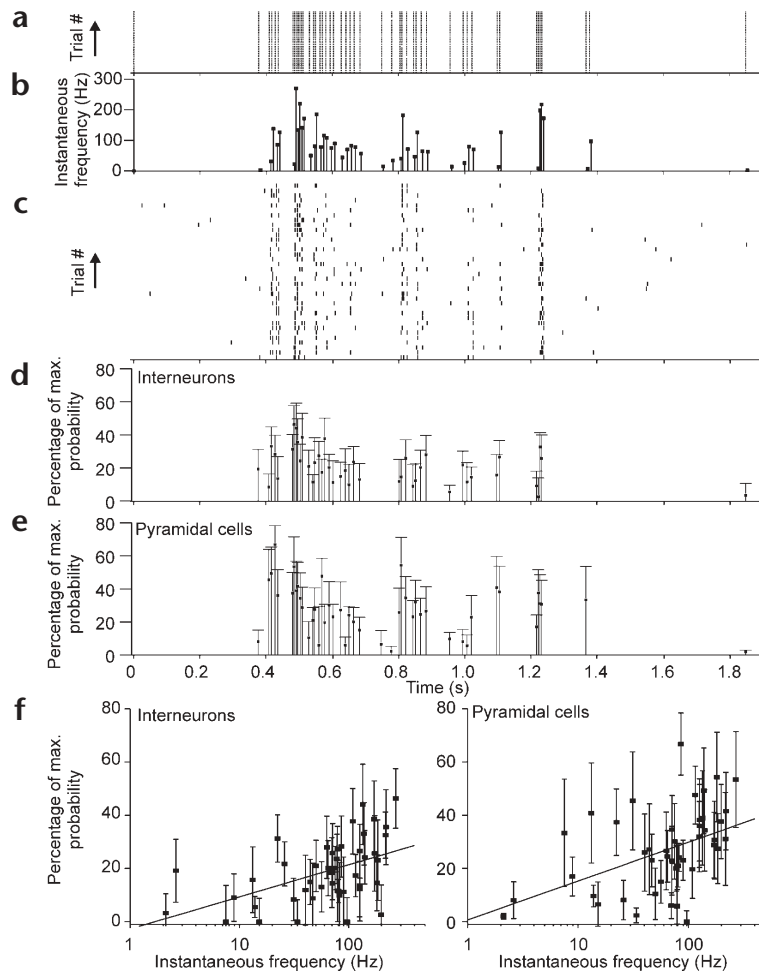


**Fig. 5.** Spike transmission from a granule cell to CA3c during physiological granule cell firing patterns. (a) Rastergram of 36 trials of granule cell action potentials evoked using template recorded during exploration while the animal traversed the place field of the granule cell (Methods). (b) Instantaneous frequency (1/previous interspike interval) of the evoked granule cell activity. (c) Rastergram of the activity of a putative CA3c pyramidal neuron. (d) Mean percent of maximum spike transmission probability ( $\pm$  s.e.m.) onto interneurons as a function of each spike in the granule cell spike train ( $n = 9$ ). The probability of each unit spiking was normalized to the maximum probability for that unit and then averaged across units. (e) As in (d), but for pyramidal cells ( $n = 6$ ). (f) Mean percent of maximum spike transmission probability ( $\pm$  s.e.m.) onto interneurons ( $n = 9$ ) as a function of instantaneous frequency (1/previous interspike interval) for each spike in the granule cell train shows that higher probability of spike transmission is associated with higher frequencies. The best linear fit regression line is shown ( $R = 0.49$ ;  $P < 0.0006$ ). (g) As in (f), but for pyramidal cells ( $n = 6$ ;  $R = 0.45$ ;  $P < 0.002$ ).

ule cells and CA3 pyramidal cells strong enough to be a high-fidelity ‘detonator’ or ‘teacher’ synapse for the storage of information in the CA3 auto-associative network<sup>3,14</sup>? According to computational models, the sparse convergence of granule cell–CA3 pyramidal cell connections<sup>11</sup> and the low mean firing rates of granule cells<sup>2,22</sup> provide an ideal mechanism for increasing the storage capacity of the hippocampus<sup>23,24</sup>. Our data indicate that the mossy fiber synapses onto CA3 targets are ‘conditional detonators’ dependent on fast repetitive firing of the presynaptic granule cell. Therefore, a single granule cell can be consid-

ered a ‘teacher’ during periods of medium to high activity by precisely timing the activity of CA3 pyramidal cells with high reliability. The temporally precise activation of action potentials in CA3 pyramidal cells would provide the necessary postsynaptic depolarization for the induction of Hebbian forms of NMDA receptor-dependent plasticity at associational/commissural and very distal perforant path synapses on CA3 pyramidal cells<sup>25</sup>. Thus granule cell activity would direct or teach the CA3 network during the storage of information<sup>14,26,27</sup>.

Previous *in vitro* experiments revealed strong excitatory postsynaptic potential facilitation by mossy fibers onto CA3 pyramidal cells<sup>28</sup> and both facilitation and depression onto interneurons<sup>13,29,30</sup>. Although single granule cells discharge mossy cells of the hilus *in vitro*<sup>31</sup>, activating single mossy fibers projecting to CA3 and mimicking the physiological pharmacology of the system *in vivo* is difficult to control in the slice preparation. In our *in vivo* experiments, granule cells rarely drove their targets with single spikes, whereas high-frequency trains of spikes and patterns with short interspike intervals in trains mimicking discharge patterns in the behaving animal robustly increased spike transmission probability to both pyramidal cells and interneurons. These findings amplify the functional importance of the robust frequency facilitation observed for the mossy fiber synapses onto CA3 targets<sup>13,28,32</sup>. Furthermore, the physiological stimulation pattern data illustrates how the mossy fiber synapse, the postsynaptic cellular properties and the local CA3 network con-

the frequency of granule cell spiking. The maximum spike transmission probability increased with the frequency of granule cell discharge (Fig. 4a and c). In 4 of 5 pairs tested, 100 Hz trains (the highest frequency tested) generated the highest spike transmission probability (Fig. 4c). The frequency sensitivity and in-train dynamics of granule cell–CA3 spike transmission in Figs. 3 and 4 indicate that the observed monosynaptic effects do not result merely from the coincidence of spontaneous background activity and current-induced spiking of the single granule cell.

Granule cells of the dentate gyrus have not been reported to fire for extended periods of times at high fixed frequencies<sup>2</sup>. Therefore, we next examined whether the natural physiological pattern of activity of a single granule cell is capable of discharging CA3 targets. To mimic the situation in the behaving rat, the presynaptic granule cell firing pattern was assigned by injecting a spike train based upon a template obtained from firing of a granule cell in a behaving animal traversing the unit’s place field (Methods). As expected, high-frequency periods of the spike train were more effective in driving both pyramidal cells and interneurons than isolated spikes or low-frequency periods (Fig. 5). Longer interspike intervals were associated with lower spike transmission probabilities, in accordance with the findings using regular spike trains.

## DISCUSSION

These experiments directly address a long-standing question in hippocampal physiology: is the connection between single gran-

ule cells and CA3 pyramidal cells strong enough to be a high-fidelity ‘detonator’ or ‘teacher’ synapse for the storage of information in the CA3 auto-associative network<sup>3,14</sup>? According to computational models, the sparse convergence of granule cell–CA3 pyramidal cell connections<sup>11</sup> and the low mean firing rates of granule cells<sup>2,22</sup> provide an ideal mechanism for increasing the storage capacity of the hippocampus<sup>23,24</sup>. Our data indicate that the mossy fiber synapses onto CA3 targets are ‘conditional detonators’ dependent on fast repetitive firing of the presynaptic granule cell. Therefore, a single granule cell can be consid-

nections all work together to generate a specific pattern of output in CA3 pyramidal cells that is dependent on, yet different from, the granule cell input.

The requirement for trains of spikes to evoke spike transmission between granule cells and CA3 is distinctly different from spike transmission between pyramidal cells and interneurons in CA1. In contrast to the granule cell–CA3 connection, single CA1 pyramidal cell spikes or low frequency trains (less than 20 Hz) are most effective in driving nearby interneurons, and the mean probability of spike transmission decreases during high-frequency trains<sup>33</sup>.

Our findings indicate that the spike number and frequency-dependent recruitment of the postsynaptic discharge is an effective mechanism to vary the time delay between the onset of granule cell activity and target neuron activity. Variable spike transmission delay lines are suggested to be critical for encoding information in computational models<sup>34,35</sup>. In the case of the mossy fiber input to CA3, this property can be thought of as a programmable delay line, in which the timing of spiking onset in CA3 varies by an order of magnitude as a function of the short-term firing rate of granule cells. For example, if entorhinal input evoked a period of 50 Hz firing in a granule cell, then the targets of that granule cell would have the highest probability of firing ~200 ms from the onset of the granule cell activity. However, if entorhinal input evoked 100 Hz firing in a granule cell, then the highest probability of CA3 activation would occur ~40 ms later. Such a mechanism could convert the spike frequency of granule cells to precise timing of CA3 target neurons during the theta cycle<sup>22,24</sup>. In addition, granule cells with a similar magnitude of activation will discharge CA3 targets together in time and thereby may increase their mutual connectivity<sup>15,16,36</sup>. Similarly, the delayed activation of CA3 pyramidal cells would be associated with dendritic back-propagating action potentials that may then facilitate potentiation of direct entorhinal inputs to CA3. This conversion of frequency to spike timing could be used to encode sequences such as an animal's trajectory through an environment<sup>22,37,38</sup>.

## METHODS

**Subjects and surgery.** Sixty-nine Sprague–Dawley rats (Hilltop Laboratories, Scottsdale, Pennsylvania, or Zivic Miller laboratories, Zellenople, Pennsylvania), 300–500 g, were anesthetized with urethane (1.5 g/kg) and placed in a stereotaxic frame. Urethane anesthesia was chosen for both the stability of the plane of anesthesia and because all known hippocampal network patterns are preserved under this anesthetic<sup>39,40</sup>. However, because urethane potentiates GABA<sub>A</sub> currents and depresses glutamate currents<sup>41</sup>, the results presented here must eventually be confirmed in the drug-free animal. All animals were treated in accordance with experimental protocols approved by the Rutgers University Animal Care and Use Committee.

**Electrophysiology.** Extracellular units were recorded using three-shank silicon tetrodes placed in the CA3c pyramidal layer. Extracellular signals were high-pass filtered (1 Hz) and amplified (1000×) using a multi-channel amplifier (Sensorium, Inc. Charlotte, Vermont). Intracellular recordings and current injections were achieved using sharp glass micropipettes (final resistance 60–140 MΩ), filled with 1 M potassium acetate and 2% biocytin, and a DC amplifier (Axoclamp-2A, Axon Instruments, Union City, California). Current injections were either square or positively offset sine waves ( $-\pi/2 - 3\pi/2$ ). Biocytin was injected intracellularly using positive current steps after each experiment and subsequently developed using diaminobenzidine. All data were digitized at 20 kHz and stored on computer disk for later analysis. Unit clustering was done using an in-house software package as described based upon principal component measurements of the extracellular units<sup>19,42</sup>. Three criteria were used to separate pyramidal cells and interneurons: spike waveform asymmetry, half-width of the spike and, when available, the

first moment of the autocorrelogram (Fig. 1; ref. 19). The existence of a monosynaptic connection was determined from the cross-correlation between the granule cell action potential peaks and the spikes from each unit. Spike transmission probability was defined as the probability of finding a unit spike in the 6 ms following the granule cell action potential. The background probability (calculated via shuffling) was subtracted from all reported probability values<sup>19</sup>. An obvious caveat of this method is that it fails to detect weak monosynaptic connections due to the absence of driven spikes. Thus, our findings may be biased for estimating strong connections.

**Physiological firing patterns.** The physiological granule cell firing pattern used in Fig. 5 was obtained from a mouse freely exploring a 40 × 40 cm open field. The selected unit is considered a 'place cell'<sup>43</sup> because it was activated selectively in a limited portion of the experimental apparatus. The unit had a low overall mean rate of 1.7 Hz and a high (26 Hz) in-field firing rate. A single representative 1.8-s period of activity when the animal traversed the place field was selected as a template of physiological activity. This sequence of spike times was converted into an analog waveform for controlling the injection of intracellular current into the granule cells. Each unit spike was converted to a sine wave pulse ~5 ms in duration and 2–3 nA in amplitude. The amplitude of the pulse was adjusted at the start of the experiment so that single action potentials were reliably elicited in the granule cell for every sine pulse (Fig. 5a). The entire 1.8-s spike train was repeatedly injected every 5 s. We used sine wave pulses to reduce the large stimulus artifacts associated with injecting large-amplitude square wave steps. The absence of the stimulus artifacts simplified detecting and measuring the intracellular action potentials evoked by the spike train.

## Acknowledgments

This work was supported by grants from the National Institutes of Health (NS34994, MH54671, MH12403, NS43157, 5P41RR009754).

## Competing interests statement

The authors declare that they have no competing financial interests.

RECEIVED 13 MAY; ACCEPTED 7 JUNE 2002

- Collier, T. J., Miller, J. S., Travis, J. & Routtenberg, A. Dentate gyrus granule cells and memory: electrical stimulation disrupts memory for places rewarded. *Behav. Neural Biol.* **34**, 227–239 (1982).
- Jung, M. W. & McNaughton, B. L. Spatial selectivity of unit activity in the hippocampal granular layer. *Hippocampus* **3**, 165–182 (1993).
- Rolls, E. T. in *Neural Models of Plasticity* (eds. Byrne, J. H. & Berry, W. O.) 240–265 (Academic, San Diego, 1989).
- Sloviter, R. S. The functional organization of the hippocampal dentate gyrus and its relevance to the pathogenesis of temporal lobe epilepsy. *Ann. Neurol.* **35**, 640–654 (1994).
- Mody, I., Lambert, J. D. & Heinemann, U. Low extracellular magnesium induces epileptiform activity and spreading depression in rat hippocampal slices. *J. Neurophysiol.* **57**, 869–888 (1987).
- Lothman, E. W., Stringer, J. L. & Bertram, E. H. in *The Dentate Gyrus and its Role in Seizures* (eds. Ribak, C. E., Gall, C. M. & Mody, I.) 301–313 (Elsevier, Amsterdam, 1992).
- Boss, B. D., Peterson, G. M. & Cowan, W. M. On the number of neurons in the dentate gyrus of the rat. *Brain Res.* **338**, 144–150 (1985).
- Amaral, D. G., Ishizuka, N. & Claiborne, B. Neurons, numbers and the hippocampal network. *Prog. Brain Res.* **83**, 1–11 (1990).
- Amaral, D. G. & Dent, J. A. Development of the mossy fibers of the dentate gyrus: I. A light and electron microscopic study of the mossy fibers and their expansions. *J. Comp. Neurol.* **195**, 51–86 (1981).
- Frotscher, M., Soriano, E. & Misgeld, U. Divergence of hippocampal mossy fibers. *Synapse* **16**, 148–160 (1994).
- Acsady, L., Kamondi, A., Sik, A., Freund, T. & Buzsáki, G. GABAergic cells are the major postsynaptic targets of mossy fibers in the rat hippocampus. *J. Neurosci.* **18**, 3386–3403 (1998).
- Maccaferri, G., Toth, K. & McBain, C. J. Target-specific expression of presynaptic mossy fiber plasticity. *Science* **279**, 1368–1370 (1998).
- Toth, K., Soares, G., Lawrence, J. J., Phillips-Tansey, E. & McBain, C. J. Differential mechanisms of transmission at three types of mossy fiber synapse. *J. Neurosci.* **20**, 8279–8289 (2000).
- McNaughton, B. L. & Morris, R. G. M. Hippocampal synaptic enhancement and information storage within a distributed memory system. *Trends Neurosci.* **10**, 408–415 (1987).



15. Markram, H., Lubke, J., Frotscher, M. & Sakmann, B. Regulation of synaptic efficacy by coincidence of postsynaptic APs and EPSPs. *Science* 275, 213–215 (1997).
16. Magee, J. C. & Johnston, D. A synaptically controlled, associative signal for Hebbian plasticity in hippocampal neurons. *Science* 275, 209–213 (1997).
17. Henze, D. A., Urban, N. N. & Barrionuevo, G. The multifarious hippocampal mossy fiber pathway: a review. *Neuroscience* 98, 407–427 (2000).
18. Henze, D. A. *et al.* Intracellular features predicted by extracellular recordings in the hippocampus *in vivo*. *J. Neurophysiol.* 84, 390–400 (2000).
19. Csicsvari, J., Hirase, H., Czurko, A. & Buzsáki, G. Reliability and state dependence of pyramidal cell-interneuron synapses in the hippocampus: an ensemble approach in the behaving rat. *Neuron* 21, 179–189 (1998).
20. Ranck, J. B. Jr. Studies on single neurons in dorsal hippocampal formation and septum in unrestrained rats. I. Behavioral correlates and firing repertoires. *Exp. Neurol.* 41, 461–531 (1973).
21. Galarreta, M. & Hestrin, S. Spike transmission and synchrony detection in networks of GABAergic interneurons. *Science* 292, 2295–2299 (2001).
22. Skaggs, W. E., McNaughton, B. L., Wilson, M. A. & Barnes, C. A. Theta phase precession in hippocampal neuronal populations and the compression of temporal sequences. *Hippocampus* 6, 149–172 (1996).
23. Rolls, E. T. In *The Computing Neuron* (eds Durbin, R., Miall, C. & Mitchison, G.) 125–159 (Addison-Wesley, Wokingham, 1989).
24. Lisman, J. E. Relating hippocampal circuitry to function: recall of memory sequences by reciprocal dentate-CA3 interactions. *Neuron* 22, 233–242 (1999).
25. Paulsen, O. & Sejnowski, T. J. Natural patterns of activity and long-term synaptic plasticity. *Curr. Opin. Neurobiol.* 10, 172–179 (2000).
26. Buzsáki, G. Two-stage model of memory trace formation: a role for “noisy” brain states. *Neurosci.* 31, 551–570 (1989).
27. Chattarji, S., Stanton, P. K. & Sejnowski, T. J. Commissural synapses, but not mossy fiber synapses, in hippocampal field CA3 exhibit associative long-term potentiation and depression. *Brain Res.* 495, 145–150 (1989).
28. Salin, P. A., Scanziani, M., Malenka, R. C. & Nicoll, R. A. Distinct short-term plasticity at two excitatory synapses in the hippocampus. *Proc. Natl. Acad. Sci. USA* 93, 13304–13309 (1996).
29. Alle, H., Jonas, P. & Geiger, J. R. PTP and LTP at a hippocampal mossy fiber-interneuron synapse. *Proc. Natl. Acad. Sci. USA* 98, 14708–14713 (2001).
30. Doherty, J. & Dingledine, R. Reduced excitatory drive onto interneurons in the dentate gyrus after status epilepticus. *J. Neurosci.* 21, 2048–2057 (2001).
31. Scharfman, H. E., Kunkel, D. D. & Schwartzkroin, P. A. Synaptic connections of dentate granule cells and hilar neurons: results of paired intracellular recordings and intracellular horseradish peroxidase injections. *Neuroscience* 37, 693–707 (1990).
32. Urban, N. N., Henze, D. A. & Barrionuevo, G. Revisiting the role of the hippocampal mossy fiber synapse. *Hippocampus* 11, 408–417 (2001).
33. Marshall, L. *et al.* Hippocampal pyramidal cell-interneuron spike transmission is frequency dependent and responsible for place modulation of interneuron discharge. *J. Neurosci.* 22, RC197 (2002).
34. Lorincz, A. & Buzsáki, G. Two-phase computational model training long-term memories in the entorhinal-hippocampal region. *Ann. NY Acad. Sci.* 911, 83–111 (2000).
35. Tank, D. W. & Hopfield, J. J. Neural computation by concentrating information in time. *Proc. Natl. Acad. Sci. USA* 84, 1896–1900 (1987).
36. Bi, G. Q. & Poo, M. M. Synaptic modifications in cultured hippocampal neurons: dependence on spike timing, synaptic strength, and postsynaptic cell type. *J. Neurosci.* 18, 10464–10472 (1998).
37. O’Keefe, J. & Recce, M. L. Phase relationship between hippocampal place units and the EEG theta rhythm. *Hippocampus* 3, 317–330 (1993).
38. Harris, K. D. *et al.* Spike train dynamics predicts theta-related phase precession in hippocampal pyramidal cells. *Nature* (in press).
39. Vanderwolf, C. H. Cerebral activity and behavior: control by central cholinergic and serotonergic systems. *Int. Rev. Neurobiol.* 30, 225–340 (1988).
40. Ylinen, A. *et al.* Sharp wave-associated high-frequency oscillation (200 Hz) in the intact hippocampus: network and intracellular mechanisms. *J. Neurosci.* 15, 30–46 (1995).
41. Hara, K. & Harris, R. A. The anesthetic mechanism of urethane: the effects on neurotransmitter-gated ion channels. *Anesth. Analg.* 94, 313–318 (2002).
42. Harris, K. D., Henze, D. A., Csicsvari, J., Hirase, H. & Buzsáki, G. Accuracy of tetrode spike separation as determined by simultaneous intracellular and extracellular measurements. *J. Neurophysiol.* 84, 401–414 (2000).
43. O’Keefe, J. & Dostrovsky, J. The hippocampus as a spatial map. Preliminary evidence from unit activity in the freely-moving rat. *Brain Res.* 34, 171–175 (1971).